Design and Performance Analysis of Hybrid Controller for Self Tuning Filter Based Solar Integrated UPQC

Koganti Srilakshmi* (iD), Uday kumar Neereti ** (iD) Yeswanth Kumar Alapati *** (iD), B. Rajagopal Reddy **** (iD), Sravanthy Gaddameedhi* (iD), M. Sai Krishna * (iD), V.Vishwanath * (iD)

*Department of Electrical Engineering, Sreenidhi Institute of Science and Technology, Hyderabad, Telangana, 501301.

**Department of Electrical Engineering, Vasavi College of Engineering, Hyderabad, Telangana, India

*** Department of Information Technology, R.V.R & J.C. college of Engineering, Guntur, Aandhra Pradesh, 522019.

**** Department of Electrical Engineering, Vardhaman College of Engineering, Hyderabad, Telangana, 501218.

(kogantisrilakshmi29@gmail.com, uday4318@gmail.com, alapatimail@gmail.com, b.rajagopalreddy@vardhaman.org, sravanthi314@gmail.com, malekarsaikrishna@gmail.com, vishwanath@gmail.com)

‡
Corresponding Author: Koganti Srilakshmi, Sreenidhi Institute of Science and Technology, Tel: +91-8885851666, kogantisrilakshmi29@gmail.com.

Abstract: The non-linear behavior of power electronics based devices leads to the power quality (PQ) issues. This paper develops an artificial intelligence hybrid controller for a unified power quality conditioner (UPQC) integrated with solar Photo-voltaic (SPV) system based on p-q theory. The p-q theory is optimized by using self-tuning filter (STF) without using any low pass filters (LPF's) or phased locked loop (PLL). The UPQC comprises a series and a shunt voltage source converter, connected with a dc link. The hybrid controller adapts both the properties of the Fuzzy Logic controller (FL-C) and artificial neural network (ANN). The prime objectives of the proposed work are minimization of harmonics in current waveforms and power factor improvement, rapid action for DC-link voltage balancing, elimination of sag/swell, distortions in the source voltage, and suitable compensation for unbalanced networks. The performance analysis of the proposed controller was carried out with four different test cases for various combinations of loads and comparative analysis was done with those of existing methods like proportional integral controller (PI-C), sliding mode controller (SM-C), and FL-C. The proposed method reduces THD from 22.67% to 3.42% and improves power factor from 0.7144 to 0.988. The results obtained by MATLAB/SIMULINK software shows the effectiveness of the proposed method

Keywords- Power quality, UPQC, FL-C, PI-C, PWM, solar power generation, battery storage system, ANN

1. Introduction

The deterioration of power quality (PQ) referring to the quality of voltage and current such as voltage sags/-swells, harmonics, interruptions, flickers, etc., is primarily due to the ever-growing usage of electric gadgets and nonlinear loads. The total harmonic distortion (THD) is an important measure of PQ and must be kept as minimum as possible. Lower THD helps in improving the efficiency, power factor, and overall life of equipment [1]. A novel synchronous-reference frame (SRF)-based controller was developed to UPQC for 3ɸ-4wire distribution network in order to mitigate PQ issues [2]. Moreover, the development of intricate algorithms enables online control of active power filters and UPQCs through different controllers such as proportional-integral controller (PI-C), Fuzzy logic controller (FL-C), and artificial neural networks (ANN) [3-6] for enhancing their dynamic performances with dynamically varying nonlinear loads.

The solar PV integrated UPQC was developed and its performance was investigated with the goal of minimizing the THD, voltage distortions by extracting maximum power [7]. Various Intelligent Control structures employing fuzzy logic and neural networks for improving power quality in the distribution system was outlined [8]. A fuzzy control was employed for enhancing the

performances of the UPQC in improving the PQ of the power system [9]. FLC based UPQC was presented to minimize the power quality issues and comparative analysis was carried out for both with and without UPQC) [10]. The Predictive phase dispersion modulation technique was developed for the Cascaded H-Bridge Multi-Level Inverter based UPQC with the objective of compensating the voltage sag/swell, current harmonics, and maintains constant DC-Link voltage [11].

The adaptive distributed power control method was developed for the two H-connected setup with eight switches of 3-φ UPQC with the aim of eliminating THD, voltage distortions [12]. PV/wind/PEMFCS fed multi-level cascade UPQC was developed with the view of minimizing supply voltage distortions and THD [13]. THD mitigation with UPQC at steel plant for induction-furnace load was investigated and to shows its superiority the comparative analysis was carried out with synchronous compensator [14]. ANFIS technique based solar integrated UPQC was designed for power quality improvement and performance analysis was carried out for different load and supply conditions [15]. Though several methods were suggested in literature, there is still a scope for developing new techniques and controllers for effectively mitigating the PQ issues. The benefits and challenges of integrating the renewable energy sources into the grid and their control strategies was studied [16]. The effects on the smart grid technologies on the national grid were highlighted and few suggestions were also given to convert conventional grid into smart grid [17]. The comparison between P & O and PSO algorithms to get MPP for the PV system was studied for solar irradiation changes [18]. Experimental set-up of isolated boost full bridge DC-DC converter was investigated along with a set of low loss active snubber circuit [19]. Integration of renewable sources to micro grid for MPPT was studies with power management [20]. High voltage isolated ACDC converters were developed based on the modular technology [21]. FDNE based method was developed based on online least square identification algorithm along with digital simulators [22]. Fuzzy logic controller was suggested for PV-MPPT to improve the overall performance by maximum power point tracking [23].

In this paper, a hybrid controller involving FL-C and ANN control for STF control based UPQC with solar PV (SPV) system has been proposed with a view of lowering the THD and improving the power factor under unbalanced source voltage with sag/swell and harmonic loading conditions. The performances of the proposed Neuro-fuzzy hybrid controller (NFHC) for STF based UPQC with SPV (U-SPV) for a test distribution system with four different test cases have been studied and compared with existing and conventional PI controllers. Section 2 designs the components of proposed UPQC, section 3 discusses the p-q control STF for UPQC and proposed NFHC, Section 4 provides results and discussions, and lastly section5 gives the conclusion.
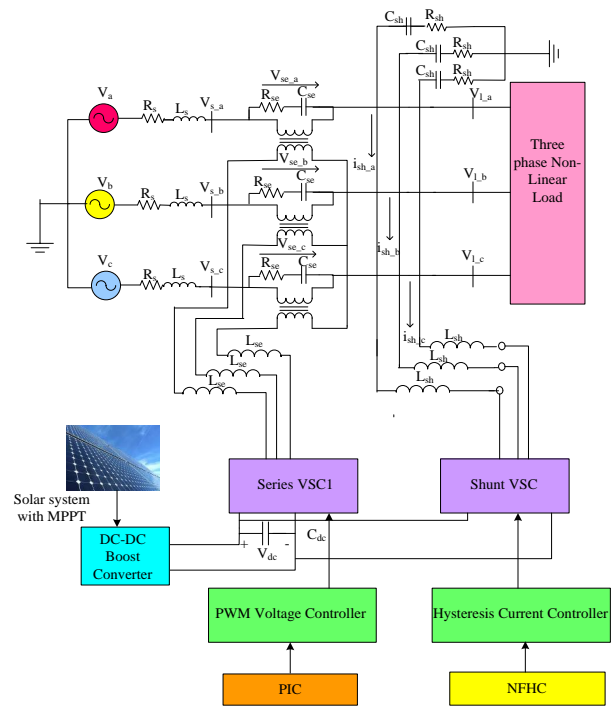

Fig. 1. Structure of UPQC with SP and BS (U-SPV)

2. Proposed U-SPV

Fig.1 illustrates the structure of UPQC supported with a Battery system (BS) and solar power (SP). The is coupled to the DC-link of UPQC via a boost converter. This work proposes NFHC for exploiting both the properties of fuzzy logic controller (FL-C) and artificial neural network (ANN). V_a , V_b , V_c are the grid voltages, V_{S_a} , V_{S_b} , V_{S_c} are bus voltages at the source side, R_s , L_S are source resistance, and inductance. UPQC comprises both series converter (SC) and shunt converter (SHC). The SC is a 3φ- PWM voltage source converter (VSC), which mitigates voltage sags/ swells, distortions, and supply voltage unbalances. Subsequently, the series RLC filter comprising of resistor R_{se} , inductor L_{se} and capacitor C_{se} is connected to prevent the flow of switching ripples.

Similarly, the transformers are connected to provide isolation between SC and the power line. It injects compensating voltage into the grid. The SHC consists of a 3φ- hysteresis current control, which is connected through a resistance R_{sh} , interfacing inductor L_{sh} , capacitance C_{sh} to provide isolation between the SHC and power line. The purpose of SHC is to diminish the current harmonics and to maintain control the dc capacitor voltage (V_{dc}) by injecting suitable current i_{sh} . The balanced 3φ rectifier load, 3φ unbalanced R-L load, and induction furnace load has been taken in the proposed work. The proposed UPQC specifications are exhibited in Table- 3.

Table 1. SPV ratings

| Device	Parameters	Values
Solar-PV panel (SPR-215-WHT-U)	Open-circuit voltage	48.3 V
	Short-circuit current	5.8 A
	Voltage/current ratings at max power output	39.80 V /5.40A
	Total parallel cells	11
	Total series cells	18

The SPV support the DC-bus through a DC-DC boost converter for improving the stability of the UPQC in compensating PQ problems as shown in Fig. 2. The SPV ratings are given in table 1. The power balance Eq. of this arrangement is given by Eq. (1).

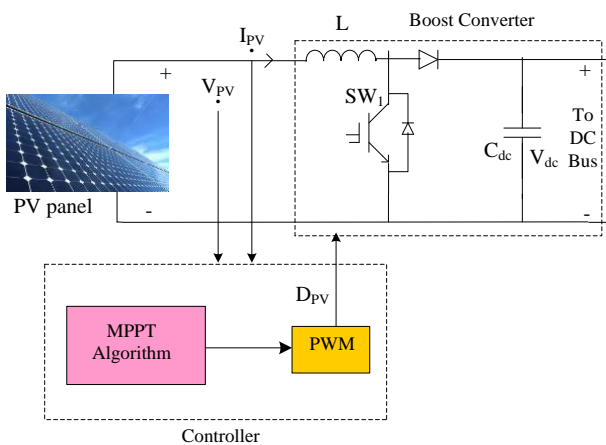$$P_{PV} - P_{dclink} = 0 \quad (1)$$

Where,

P_{PV} denote the power supplied by Solar .

P_{dclink} represents the load at DC-link.
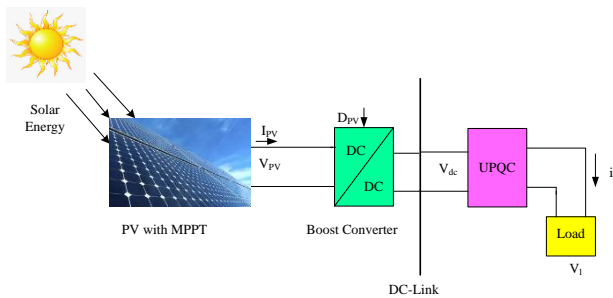
Fig. 2. Schematic Diagram of external support of DC-Link

Fig. 3. Solar PV system with controller

2.1 Solar photo-voltaic system

The solar power system is used to convert solar energy into electrical energy. The SPV controller consists of a three main parts: solar-PV panel with MPPT, and boost converter (BC) as shown in Fig.3. The production of electrical energy is decided by the solar-irradiation on PV cells. The main purpose of applying MPPT is to extract

maximum output voltage from the PV cell under the precise irradiance/ temperature. The output power P_{PV} of the PV panel can be calculated by Eq. (2)

$$P_{PV} = V_{PV}.I_{PV} \quad (2)$$

Where, V_{PV}, and I_{PV} are the solar PV panel output Voltage and Current. In this work, MPPT adopts the well known Perturb-and-observes (P & O) algorithm to control the duty-cycle (D) of the boost-converter. The ratings of SPV are given in Table-1.

3. Control Strategy

According to p-q theory to compensate current harmonics and voltage distortions, first they are transformed into the clarke's reference. Later, harmonics and fundamental components (FC) are alienated and the reference currents are produced for the hysteresis band controller. Generally, the conventional system has SHAPF control, PLL and SAPF control. Where, a PLL is used to split the positive sequence components from the unbalanced/ distortional source voltage but in the suggested control method a STF is used for it. In addition, STF also does the work of LPFs and HPFs for splitting the FC of current. So, the proposed control consists of a STF, SHAPF and a SAPF.

3.1 Modeling of STF

Hong-Sock has calculated integral in the synchronous reference frame (SRF) given in Eq. (3)

$$V_{xy}(t) = e^{j\omega t} \int e^{-j\omega t} U_{xy}(t)dt \quad (3)$$

Where, U_{xy} and V_{xy} are before and after integration instantaneous-signals in the SRF. By applying the Laplace transformation on Eq.3, the transfer function $H(s)$ is given in Eq.4

$$H(s) = \frac{V_{xy}(s)}{U_{xy}(s)} = \frac{s + j\omega}{s^2 + \omega^2} \quad (4)$$

In order to get STF with a cut off frequency from $H(s)$, a constant parameter k is introduced [ ]. Thus, $H(s)$ is as given in Eq.5

$$H(s) = \frac{V_{xy}(s)}{U_{xy}(s)} = \frac{k(s + k) + j\omega_n}{(s + k)^2 + \omega_n^2} \quad (5)$$

By swapping $U_{xy}(s)$ by $x_{\alpha\beta}(s)$ and $U_{xy}(s)$ by $x'_{\alpha\beta}(s)$, Eq. (6)-(7) is obtained:

$$x'_\alpha = (\frac{k}{s}[x_\alpha(s) - x'_\alpha(s)] - \frac{\omega_n}{s}.x'_\beta(s)) \quad (6)$$

$$x'_\beta = (\frac{k}{s}[x_\beta(s) - x'_\beta(s)] - \frac{\omega_n}{s}.x'_\alpha(s)) \quad (7)$$

Where, ω_n is the expected frequency of output, and k is the filter's gain. If the value of k increases the accuracy

of extracting the desired component increases and vice-versa. Therefore, by using a STF, distortional signals of both voltage and current can be acquired without any change in there magnitude and phase angle. The modeled control structure of a STF is shown in Fig. 4 [33].
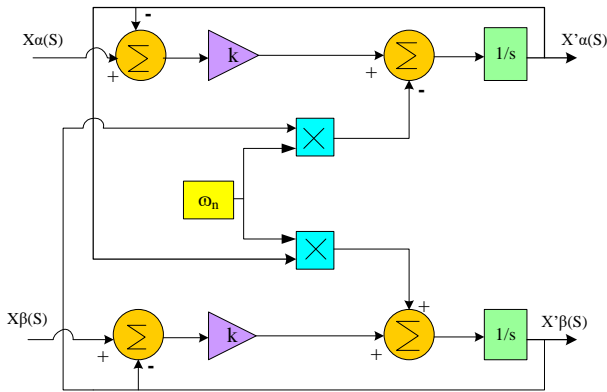

Fig. 4. The control structure of STF

3.2 Shunt Controller

The role of the shunt-VSC is to suppress the supply harmonic currents by injecting suitable compensating current at PCC and to maintain constant DC-Link voltage. The hybrid controller for shunt-VSC adapts (i) abc-αβ and αβ-abc domain conversions; (ii) NFHC is used for reducing current harmonics and maintaining constant DC-link voltage. NFHC compares DC-Link voltage with a reference DC-Link voltage and transforms the error injected into axis. The schematic diagram of the NFHC is depicted in Fig. 5. The transformation of currents from abc to αβ and then again to abc domain including STF, the design of the NFHC control part is explained below:
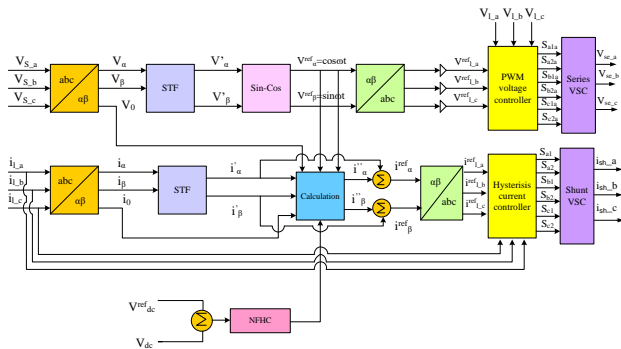

Fig. 5. NFHC for Shunt Converter

The SHAPF is controlled by p-q theory. According to it, currents are transferred to α - β - 0 coordinates by using Eq.8

$$\begin{bmatrix} i_0 \\ i_\alpha \\ i_\beta \end{bmatrix} = \begin{bmatrix} \frac{1}{\sqrt{2}} & \frac{1}{\sqrt{2}} & \frac{1}{\sqrt{2}} \\ 1 & -\frac{1}{2} & -\frac{1}{2} \\ 0 & \frac{\sqrt{3}}{2} & -\frac{\sqrt{3}}{2} \end{bmatrix} \begin{bmatrix} i_{l\_a} \\ i_{l\_b} \\ i_{l\_c} \end{bmatrix} \quad (8)$$

The currents are transferred to the Clark's plane and then given to STF. The STF output is the FC (i'_α and i'_β) contains the FC of both active-power (AP) and reactive-powers (RP). For the total compensation of the RP is given in Eq. 9. The switching loss (p_{Loss}) are injected into main axis. In addition, for the constant maintain of DC-Link voltage V_{dc} is compared with the $V^{ref}{}_{dc}$, and then obtained error is injected by NFHC. Then the reference currents are obtained by Eq. 10-14.

$$q' = i'_\beta \, v'_\alpha - i'_\alpha \, v'_\beta \quad (9)$$

$$p_0 = v_0 i_0 \quad (10)$$

$$\begin{bmatrix} i'_\alpha \\ i'_\beta \end{bmatrix} = \frac{1}{v'^2{}_\alpha + v'^2{}_\beta} \begin{bmatrix} v'_\alpha & -v'_\beta \\ v'_\beta & v'_\alpha \end{bmatrix} \begin{bmatrix} p_{Loss} + p_0 \\ -q' \end{bmatrix} \quad (11)$$

$$i^{ref}{}_\alpha = i'_\alpha - i''{}_\alpha \quad (12)$$

$$i^{ref}{}_\beta = i'_\beta - i''{}_\beta \quad (13)$$

$$\begin{bmatrix} i_l{}^{ref}{}_a \\ i_l{}^{ref}{}_b \\ i_l{}^{ref}{}_c \end{bmatrix} = \sqrt{\frac{2}{3}} \begin{bmatrix} 1 & 0 \\ -\frac{1}{2} & \frac{\sqrt{3}}{2} \\ -\frac{1}{2} & -\frac{\sqrt{3}}{2} \end{bmatrix} \begin{bmatrix} i^{ref}{}_\alpha \\ i^{ref}{}_\beta \end{bmatrix} \quad (14)$$

These reference load currents are compared with load currents and then obtained errors are given to a hysteresis controller in order to generate switching signals of SHAPF.

3.2.1 Proposed NFHC

The NFHC is a combination of a fuzzy logic control mechanism whose process is inspired by the neural network technique. The fuzzy logic controller is based upon mathematical reasoning that works on designated linguistic rules. The fuzzy logic control consist set of fuzzy rules which export the output as linguistic variables instead of numerical values. The fuzzy logic controller operates on three mechanisms fuzzification, inference, and defuzzification. Fuzzification is the process of conversion of numerical values into linguistic variables. A set of membership functions are defined to evaluate the variables. A set of membership functions (MF) are defined to evaluate the variables. Based upon the membership functions the variables take a specific linguistic value. The membership functions and the set of rules are determined at the inference stage. Based on the input, the output takes any one of the values in the defuzzification stage. The overall fuzzy controller is shown in Fig.6.

The Takagi–Sugeno fuzzy model takes error (E) and rate of the change of the error (CE) as inputs. The error is calculated by Eq. (15). Triangular MF is used for an error and change in error of the FL-C as given in Figs.8 and 9 respectively. The fuzzy variables are denoted by triangular membership functions given in Fig. 7-8 involving PSH, medium positive (PSM), PSL, ZE, NEH, medium negative (NEM) and NEL. The value of the DC link voltage takes values in-between any of these linguistic variables. The DC link voltage is made to be operated within a set of membership functions hence a total of 49 possible sets are obtained which is given in Table 2.

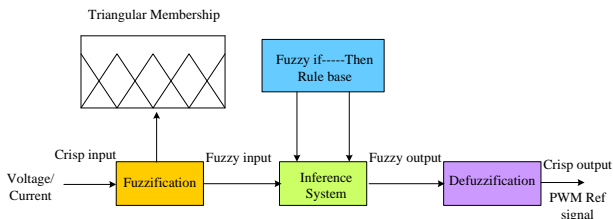$$E = V^{ref}{}_{dc} - V^{i}{}_{dc}; i = 1,2,3,4,5,6 \quad (15)$$
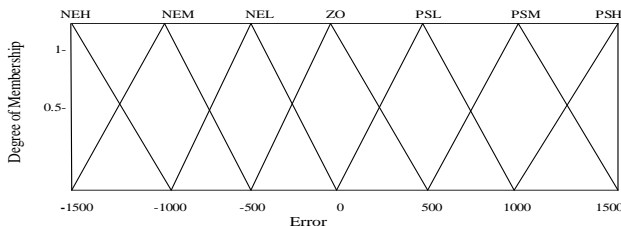

Fig. 6. Overview of Fuzzy controller

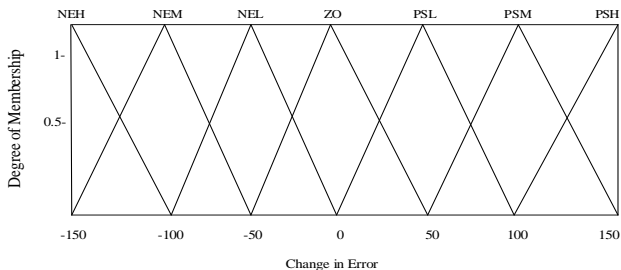**Fig. 7.** MF for "Error"

Fig. 8. MF for "Change in Error"

The neural network is an adaptive control technique that works identical to the human brain. The neural network controller can train itself based upon the different working conditions. The neural network consists of interconnected neurons which are trained to work based on requirement. The network consists of input, an output layer, and numerous hidden layers are embedded between the input and output layers. These hidden layers are allocated with specific weights and based upon the weights of the layer the priority is assigned at each stage.

Table 2. MF mapping for DC-Link voltage

E	CE						
	PSH	PSM	PSL	ZE	NEL	NEM	NEH
NEH	ZE	NEL	NEM	NEB	NEH	NEH	NEH
NEM	PSL	ZE	NEL	NEM	NEH	NEH	NEH
NEL	PSM	PSL	ZE	NES	NEM	NEH	NEH
ZE	PSH	PSM	PSL	ZE	NEL	NM	NEH
PSL	PSH	PSH	PSM	PSL	ZE	NEL	NEM
PSM	PSH	PSH	PSH	PSM	PSL	ZE	NEL
PSH	PSH	PSH	PSH	PSH	PSM	PSL	ZE

The proposed adaptive neuro-fuzzy controller is a more reliable adaptive controller that combines the functionality of both the neural network and fuzzy logic mechanism. The inputs are first trained according to the membership functions and then the inputs are fed to the neural networks and based upon the number of hidden layers the controller gets trained and output is got after proper evaluation. The overview of the proposed NFHC is shown in Fig.9. The triangular inference output is trained by the hybrid neural network algorithm to generate the optimized output. In the PV integrated UPQC system $V^{ref}{}_{dc}$ is compared with reference $V^{ref}{}_{dc}$ signal, the DC link voltage sensed from the DC link capacitor is fed to the NFHC controller. The ANN system is trained with the Levenberg-Marquardt algorithm.
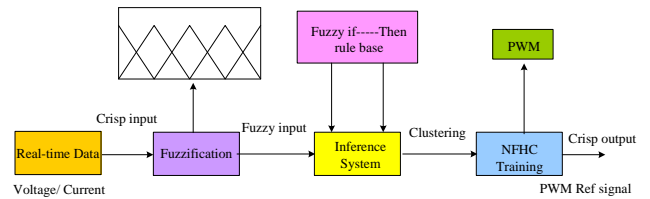

Fig. 9. Overview of NFHC

The NFHC system can be modeled mathematically as two input parameters (u and v) with an AND operator to get the output (z) can be expressed as Eq. (16).

IF u is X and v is Y, then $z = f(u,v)$ (16)

There exist five layers, consider the membership function at the fuzzification layer with first input u is expressed as $\beta_{xj}(u)$, the membership functions used is denoted by j. The AND operator is implemented in the second layer, the neurons at the second layer are given in Eq. (17).

$$w_i = \beta_{xj}(u) * \beta_{\beta yj}(v) \quad (17)$$

The third layer contributes to the normalization of the values from the second node. The normalized values in the third layer are expressed in Eq. (18).

$$w_i = \frac{w_i}{w_1 + w_2} \quad (18)$$

The self-adaptive property of the ANN controller is implemented by using the inference parameters (a_i, b_i, c_i) in the fourth node through Eq. (19).

$$\overline{w_i} f_i = \overline{w_i}(a_i u + b_i v + c_i) \quad (19)$$

The inputs get summed up at the fifth layer to generate the output given in Eq. (20).

$$f = \sum_i \overline{w_i} f_i \quad (20)$$

The block diagram representing the five layers of the NFHC system with two input parameters is as shown in Figure 10. The fuzzy rules that apply to the structure are given as Eq. (21) - (22).

If u is X_1 AND v is Y_1, then $f_1 = a_1 u + b_1 v + c_1$ (21)

If u is X_2 AND v is Y_2, then $f_2 = a_2 u + b_2 v + c_2$ (22)

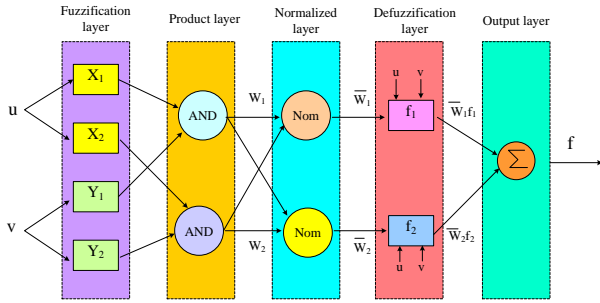The NFHC system works based on the above mathematical Equations.

Fig.10. Structure of NFHC

3.3 Series Controller

The SAPF is used for minimizing all the voltage related issues like sag, sell, and distortions. By using Eq.22 the source voltages are transferred into $\alpha - \beta - 0$ coordinates and harmonic components are separated from FC of voltage by the STF given in Eq. (23)-(25).

$$\begin{bmatrix} V_0 \\ V_\alpha \\ V_\beta \end{bmatrix} = \sqrt{\frac{2}{3}} \begin{bmatrix} \frac{1}{\sqrt{2}} & \frac{1}{\sqrt{2}} & \frac{1}{\sqrt{2}} \\ 1 & \frac{-1}{2} & \frac{-1}{2} \\ 0 & \frac{\sqrt{3}}{2} & \frac{-\sqrt{3}}{2} \end{bmatrix} \begin{bmatrix} V_{S\_a} \\ V_{S\_b} \\ V_{S\_c} \end{bmatrix} \quad (23)$$

$$V_\alpha = V'_\alpha + V^{ref}_\alpha \quad (24)$$

$$V_\beta = V'_\beta + V^{ref}_\beta \quad (25)$$

When two extreme unbalance input signals are given to STF, it will develop two identical magnitude sine-waves by Eq. (26)

$$\frac{x_\alpha(s) + x_\beta(s)}{2} = x'_\alpha(s) = x'_\beta(s) \quad (26)$$

Therefore, in order to produce the reference voltages, first $V'_\alpha(s)$ and $V'_\beta(s)$ are obtained. Later, the reference voltages in abc domain are calculated by Eq. 27.

$$\begin{bmatrix} V^{ref}_{l\_a} \\ V^{ref}_{l\_b} \\ V^{ref}_{l\_c} \end{bmatrix} = \sqrt{\frac{2}{3}} G \begin{bmatrix} 1 & 0 \\ -\frac{1}{2} & \frac{\sqrt{3}}{2} \\ -\frac{1}{2} & -\frac{\sqrt{3}}{2} \end{bmatrix} \begin{bmatrix} V'_\alpha \\ V'_\beta \end{bmatrix} \quad (27)$$

Where, G is denoted as the expected maximum value of phase voltage. The reference load voltages ($V^{ref}_{l\_a}$, $V^{ref}_{l\_b}, V^{ref}_{l\_c}$) are compared with the distorted load voltage ($V_{l\_a}, V_{l\_b}, V_{l\_c}$) and the obtained errors are supplied to the PWM voltage controller to generate the required signals for of the SAPF shown in Fig.5.

4 Results and Discussions

The proposed UPQC with SP and BS (U-SPV) was studied on a 3-φ AC distribution system. The Simulation model for the U-SPV has developed in Matlab 2016a platform is shown in Fig. 11. Four different test cases with various combinations of balanced and unbalance non-liner loads, conditions like sag/ swell, and distortions as given in Table 4, were considered for studying the performances of the U-SPV. The source voltage is considered balanced with voltage sag/ swell, disturbance for cases 1, 2 and unbalanced for case 3, 4 respectively. The results are compared with existing methods available in the literature.

The THD for source current (i_S) of the U-SPV was obtained for all the test cases and compared with those PI-C, SM-C, FL-C, and NFHC in Fig.12. The power factor (PF) at the source side of the proposed NFHC calculated by Eq. (28) for all test cases and comparison is as shown in Fig.13.

$$Powerfactor = \cos\theta * \frac{1}{\sqrt{1 + THD^2}} \quad (28)$$

Where, Θ is the measured angle between voltage and current, while $\frac{1}{\sqrt{1 + THD^2}}$ represents displacement factor.

Table 3. UPQC specifications and loads

Source	V_s : 415V ; f : 50Hz
	R_s : 0.10Ω ; L_s : 0.150mH
Series compensator	R_{se} : 1.0Ω ; L_{se} : 3.60mH ; C_{se} : 60.0 µf
Shunt compensator	R_{sh} : 0.0010Ω ; L_{sh} : 2.150mH ; C_{sh} : 1.0 µf
	VSC hysteresis controller band: 0.010A
Dc-Link	C_{dc} : 9400.00µf ; V_{dc} Voltage: 700.0V
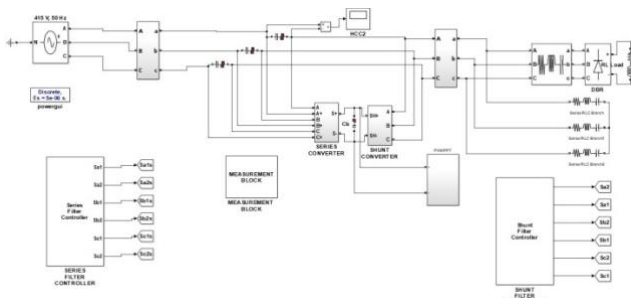
Fig. 11. Simulink model of UPVB along with test system

The source voltage (V_S), injected voltage (V_{se}), load voltage (V_l), dc-link voltage (V_{dc}), load current (i_l), injected current (i_{sh}), source current (i_S) waveforms during steady state as well as sag/swell, disturbance conditions of the U-SPV for test cases 1-3 are shown in fig. 16-18.

In case1, the voltage was sagged by 30% during the interval 0.2-0.3s and swelled by 30% during 0.4-0.5s. The voltage distortion was introduced during 0.6-0.7 s, as shown in Fig. 14(a). Moreover, the load current was non-sinusoidal but balanced with a THD of 22.67% and a PF of 0.789 due to nonlinear rectifier load is presented in Fig. 14(b). It can be seen from Fig. 14 that the U-SPV can provide a more stable load voltage and sinusoidal source current. Such enhancement in current waveforms also reflected in the THD and PF values the THD of the load current was reduced from 22.67% to 3.42%, which is smaller than those of the existing methods and the PF rose from 0.789 to 0.988 by injecting appropriate series voltages and shunt currents.

In case2, the voltage sag, swell, and disturbances introduced are similar to case1, shown in Fig. 15(a). Here, the load current was sinusoidal but unbalanced with a THD of 18.88% and a power factor of 0.623 due to nonlinear unbalanced load as presented in Fig. 15(b). It is seen that the U-SPV was able to eliminate sag/swell and disturbances effectively and reduce THD from 18.88% to 2.30% thereby improving PF value from 0.623 to 0.987 by injecting suitable shunt currents.

In case3- the unbalanced supply voltage was considered for balanced load shown in Fig. 16(a). The load current was non-sinusoidal and balanced with a THD of 11.91% and a PF of 0.875 Fig. 16(b). The NFHC is able to reduce the THD from 11.91% to 3.43% and improve PF from 0.875 to 0.992 by injecting suitable shunt currents and maintaining the voltage.

In case4- the unbalanced supply voltage was considered for unbalanced load shown in Fig. 17(a). The load current was non-sinusoidal and unbalanced with a THD of 9.26% and a PF of 0.875 Fig. 17(b). The NFHC is able to reduce the THD from 9.26% to 2.29% and improve PF from 0.875 to 0.999 by injecting suitable shunt currents

and maintaining the voltage. The THD spectrum for all test cases is as shown in Fig.19.

However, from the above studied test cases it is clearly observed that the proposed method can able to mitigate current and voltage related PQ issues efficiently for balance and unbalanced source and loads. In addition, it exhibits superior performance even during solar irradiation variation (uncertainty during cloudy condition) shown in Fig. 18.

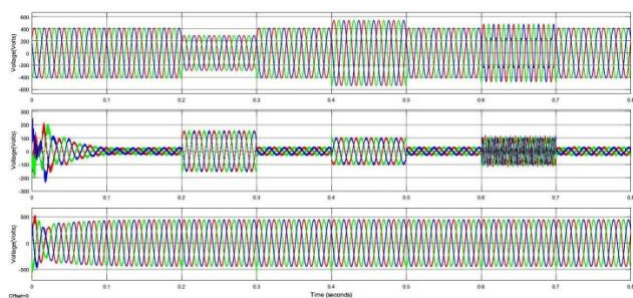**Table 4.** Test cases considered

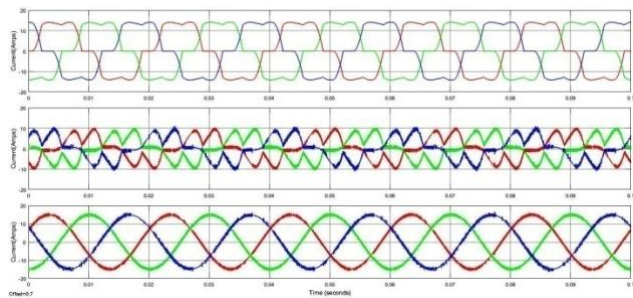| State of the system	Case1	Case2	Case3	Case4
Balanced source voltage	✓	✓		
Unbalanced source voltage			✓	✓
Voltage Sag/ Swell, Disturbance	✓	✓		
Steady state current	✓	✓	✓	✓
Steady state voltage			✓	✓
Balanced-3 φ Rectifier Load: 30.0Ω & 20.0mH	✓	✓	✓	
Unbalanced-3 φ RL Load: R: 10.0, 20.0 &15.0 Ω; L: 9.50, 10.50 & 18.50 mH.		✓		✓
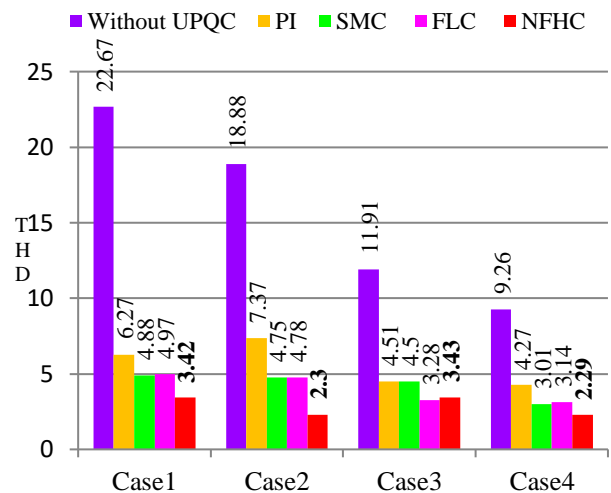
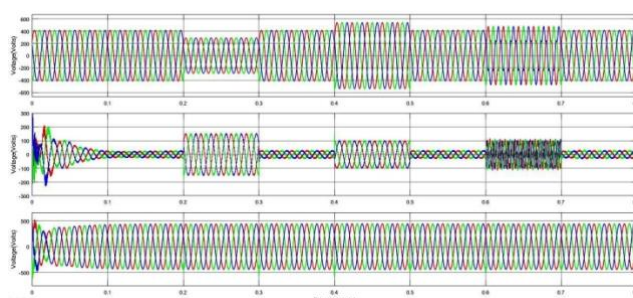**Fig. 12**. THD comparison bar chat
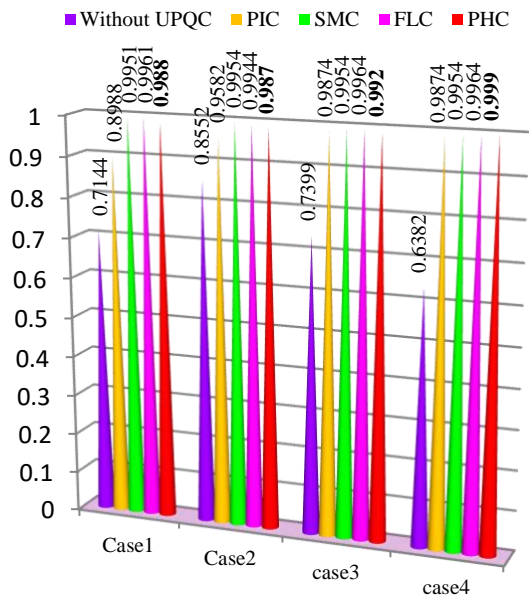
Fig. 13. PF for test cases

(a) V_S , V_{se} , V_l

(b) i_l , i_{sh} , i_S
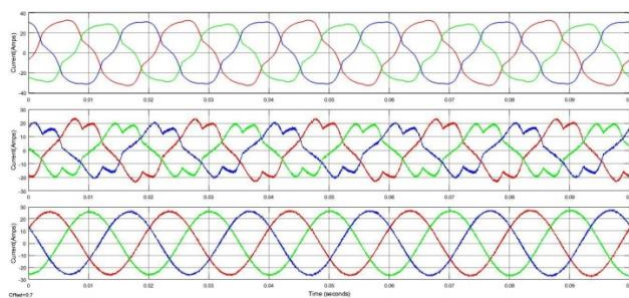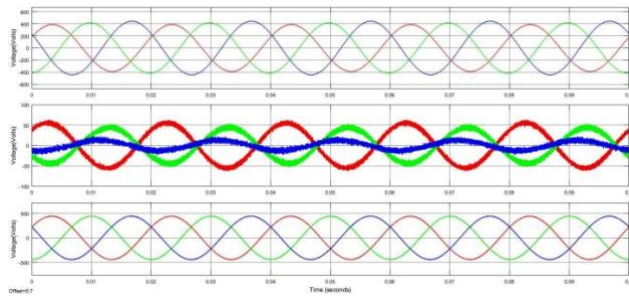
Fig. 14. Waveforms of proposed system for case-1

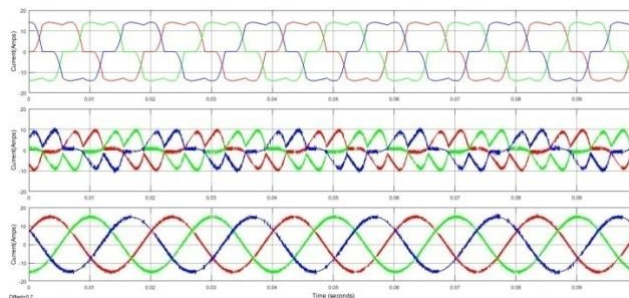
(a) V_S , V_{se} , V_l

(b) i_l , i_{sh} , i_S
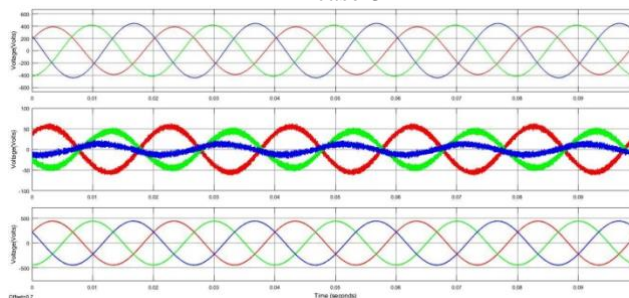
Fig. 15. Waveforms of Proposed system for case-2
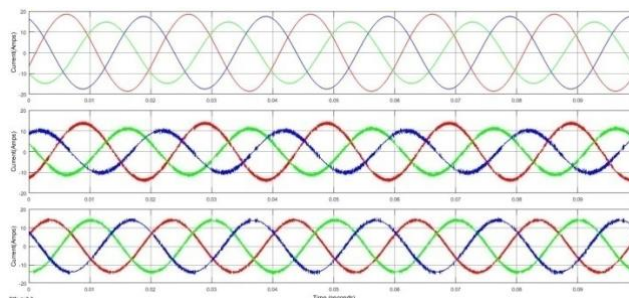

(a) V_S , V_{se} , V_l

(b) i_l , i_{sh} , i_S
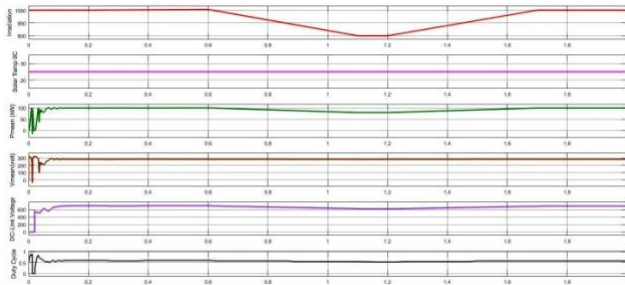
Fig. 16. Waveforms of Proposed system for case-3
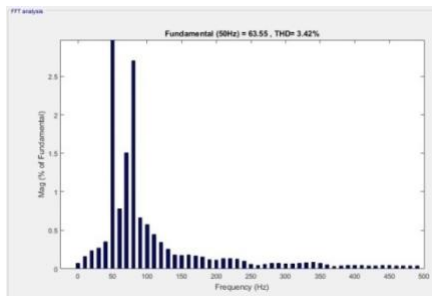

(a) V_S , V_{se} , V_l
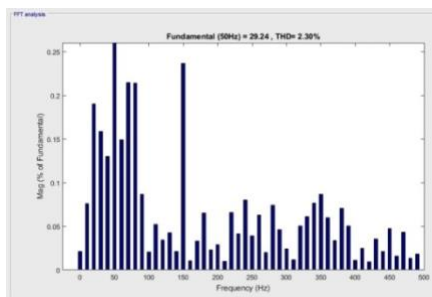

(b) i_l , i_{sh} , i_S

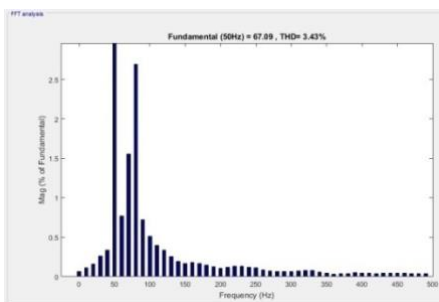**Fig. 17.** Waveforms of Proposed system for case-4

Fig. 18. Solar irradiation variation, Temperature, Solar output power, solar voltage, DC-Link voltage, Duty cycle
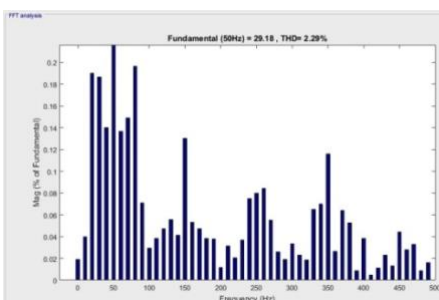

Case1

Case2

Case3

Case4

Fig. 19. THD spectrum for case studies

4. Conclusion

A hybrid controller involving FL-C and ANN controller was proposed for STF based U-SPV. The controller for SPV and design of STF with transformations were also given in addition to developing of NFHC for shunt SVC controllers with a goal of achieving fast action in maintaining dc-link voltage, eliminating sags/swells in supply voltage, minimizing the THD in load voltage and source current, and improving the power factor under balanced and unbalanced supply voltage conditions. From the study on four test cases with different load combinations, balanced and unbalanced source voltages, voltage sag and swells and distortions clearly exhibited that the NFHC was able to lower the THDs within acceptable levels and power factors almost unity. Moreover, these performances were much better than those of the existing controllers of PI-C, SM-C and FL-C. The NFHC also maintains constant DC-link voltage for all irradiation variations. The proposed model can further be studied on distribution systems with the micro-grid as future work. Moreover, the hybrid controller concept can be extended for the series VSC of UPQC.

References

1. Y. Wang, and M. Wong, "Historical Review of Parallel Hybrid Active Power Filter for Power Quality Improvement", IEEE TENCON, Jan 2015.

2. M. Kesler and E. Ozdemir, "Synchronous-Reference-Frame-Based Control Method for UPQC under Unbalanced and Distorted Load Conditions", IEEE Transactions on Industrial Electronics, Vol. 58, No. 9, pp. 3967-3975, September 2011.

3. M. Suresh and A. K. Panda, "PI and Fuzzy Logic Controller based 3-phase 4-wire Shunt active filter for mitigation of Current harmonics with Id-Iq Control Strategy", Journal Of Power Electronics, Springer, Vol. 11, No. 6, Nov 2011.

4. P. Kirawanich, and M.O.C. Robert, "Fuzzy Logic Control of an Active Power Line Conditioner", IEEE Transactions on Power Electronics, Vol. 19, No.6, Nov 2004.

5. M. Suresh and A. K. Panda, "RTDS hardware implementation and simulation of SHAF for mitigation of harmonics using p-q control strategy with PI and Fuzzy logic controllers", Frontiers of Electrical and Electronic Engineering , Springer, Vol. 7, No. 4, pp. 427–437, June 2012.

6. C.L. Hsiung, "Intelligent Neural Network-Based Fast Power System Harmonic Detection," IEEE Transactions on Industrial Electronics, Vol. 54, No. 1, pp. 43-52, Feb 2007.

7. S. Devassy, BhimSingh, "Design and Performance Analysis of Three-Phase Solar PV Integrated UPQC", IEEE 6th International Conference on Power Systems, Oct 2016.

8. P. K. Dash S. K. Panda T. H. Lee, J. X. Xu, A. Rou tray, "Fuzzy and Neural Controllers for Dynamic Systems: an Overview". Proceedings of Second

International Conference on Power Electronics and Drive Systems, pp. 810-816, May 1997.

9. G.B. Mohankumar and S. Manoharan, "Performance Analysis of Multi Converter Unified Power Quality Conditioner with Dual Feeder System using Fuzzy Logic Control", International Journal of Control and Automation, Vol. 8, No. 3, pp. 251-270. March 2015.

10. M. Almelian, I. Mohd, M. Omran and U. U.Sheikh, "Performance of unified power quality conditioner (UPQC) based on fuzzy controller for attenuating of voltage and current harmonics", IOP Conf. Series: Materials Science and Engineering, Vol.3, No.1, pp. 012-084, April 2018.

11. V. Vinothkumar, R. Kanimozhi, "Power flow control and power quality analysis in power distribution system using UPQC based cascaded multi-level inverter with predictive phase dispersion modulation method", Journal of Ambient Intelligence and Humanized Computing, Springer, Vol.12, pp. 6445–6463, 2021.

12. M. R. Mohanraj, R. Prakash, "A Unified Power Quality Conditioner for Power Quality Improvement in Distributed Generation Network Using Adaptive Distributed Power Balanced Control (ADPBC)", International Journal of Wavelets, Multi-resolution and Information Processing, Vol. 18, No. 01, pp. 1941021, 2020.

13. K. Sarker, D. Chatterjee & S. K. Goswami, "A modified PV-wind-PEMFCS-based hybrid UPQC system with combined DVR/STATCOM operation by harmonic compensation", International Journal of Modeling and Simulation, World Scientific, Vol.41, No.4, pp. 243-255, March 2020.

14. S. S. Tejinder, S. Lakhwinder, B. Gill & M. Om Parkash, "Effectiveness of UPQC in Mitigating Harmonics Generated by an Induction Furnace", Electrical Power Components and Systems, Taylor & Francis, Vol. 46, No. 6, pp. 629-636, Nov-2018.

15. S.S. Dheeban & N.B. Muthu Selvan, "ANFIS-based Power Quality Improvement by Photovoltaic Integrated UPQC at Distribution System", IETE Journal of Research, Taylor & Francis, Feb-2021.

16. F. Ayadi; I. Colak; I. Garip, H. Bulbul, "Impacts of Renewable Energy Resources in Smart Grid", 8th International Conference on Smart Grid, Paris, pp. 183-188, June 2020.

17. I. Colak; R. Bayindir, S. Sagiroglu, "The Effects of the Smart Grid System on the National Grids", 8th International Conference on Smart Grid, Paris, pp. 122-126, June 2020.

18. S. Jaber, A. M. Shakir, "Design and Simulation of a Boost-Microinverter for Optimized Photovoltaic System Performance", International Journal of Smart Grid, Vol. 5, No. 2, pp. 1-9, June 2021.

19. S. Ikeda, F. Kurokawa, "Isolated and wide input ranged boost full bridge DC-DC converter for improved resilience of renewable energy systems", San Diego, CA, USA, pp. 290-295, 5-8 Nov. 2017.

20. S. S. Dash, "Tutorial 1: Opportunities and challenges of integrating renewable energy sources in smart" 6th International Conference on Renewable Energy Research and Applications , San Diego, CA, USA, 5-8 Nov. 2017.

21. M. Tsai, C. Chu, W. Chen, "Implementation of a Serial AC/DC Converter with Modular Control Technology", 7th International Conference on Renewable Energy Research and Applications, Paris, France, pp. 245-250, Oct. 2018.

22. A. Thakallapelli, S. Ghosh; S. Kamalasadan, "Real-time frequency based reduced order modeling of large power grid" IEEE Power and Energy Society General Meeting Boston, MA, USA, 17-21 July 2016.

23. A. Belkaid, I. Colak, K. Kayisli, R. Bayindir, Improving PV System Performance Using High Efficiency Fuzzy Logic Control, 8th International Conference on Smart Grid, Paris, pp.152-156, June 2020.